Emerg Mater (2023) 6:197–209
https://doi.org/10.1007/s42247-022-00411-w

ORIGINAL ARTICLE

Development of biodegradable calcium alginate films for packaging applications

Omkar Saswat[1,2] · **Priyanka H. Maheshwari**[1,2]

Received: 17 May 2022 / Accepted: 5 September 2022 / Published online: 23 September 2022

Abstract
Plastic films have long been used for packing applications. However, the serious issues it poses to the environment has motivated the development of calcium alginate films as a prospective material for packaging purpose. The films were prepared by cross-linking sodium alginate with calcium chloride, whereby the effect of variation in the concentration of the cross-linker and the cross-linking time were studied. Several parameters like thickness, density, moisture content, water uptake degree, swelling ratio, solubilized matter in water, tensile strength, elongation %, transmittance, and biodegradability were studied to find the sample best suited for packaging application. It was found that the samples prepared with a low concentration of $CaCl_2$ (3%) while cross-linking it for 30 min resulted in uniformity with reduced moisture and water uptake and high tensile strength. Furthermore, the samples could degrade at a much faster rate as compared to polythene and even paper when tested under similar conditions.

Keywords Biodegradability · Calcium alginate · Tensile strength · Transparency · Water uptake

1 Introduction

Food packaging is an important part of the food industry. The quantity of food packaging materials is increasing by 8% annually leading to high accumulation of plastics [1] and Styrofoam (thermocol) in the environment [2], the recycling of which is less than 5%. Biologically derived resources used in the past for making food packaging [3] and serving materials (paper, dried leaves) [4], are no longer preferred owing to their weight and low durability. On the other hand, polymer materials (especially polyethylene) have become the golden touch of King Midas, which despite their various advantages, are polluting and starving our environment. Hence, researchers [5, 6] are now trying to develop alternative materials which are biodegradable and durable. Generally, polysaccharides [7], lipids, and proteins [8, 9] have been employed for the development of biodegradable packaging materials. Alginate and pectin have been used for the formation of biodegradable films, and both can be used to incorporate antimicrobial agents [9]. Sodium alginate is a polysaccharide having unique properties such as tailorable rheological [10] and gelation characteristics [11], thermal stability [12], emulsion stabilization [13], film-forming properties, biodegradability, biocompatibility, and low toxicity [14, 15]. Sodium alginate, extracted from brown algae, is a linear polysaccharide having hydrophilic characteristics. It is a combination of β-D-mannuronic (M) acid and α-L-gluronic (G) acid, joined with glycosidic (1–4) bonds [16]. Due to its low toxicity, sodium alginate has been used in various applications in the biomedical industry [17], food industry [18, 19], industrial waste treatment [20, 21], and pharmaceuticals [15, 22, 23]. Sodium alginate reacts with polyvalent metal cation especially calcium ion, to produce cross-linked material, which has been used in the food processing industries [14] and biotech industry [23, 24], and as a stabilizer for cells and enzymes.

The process of cross-linking the soluble sodium alginate with calcium to form insoluble calcium alginate can further be optimized to increase the tensile strength and elongation percentage of the later considerably [25]. Hence, the present investigation proposes to develop calcium alginate films for packaging application as a replacement for polythene which is most used for food packaging and holding. Literature have been

✉ Priyanka H. Maheshwari
hedap@nplindia.org

[1] Advanced Carbon Products & Metrology Section, CSIR–National Physical Laboratory, Dr. K. S. Krishnan Road, New Delhi-12, India

[2] Academy of Scientific and Innovative Research (AcSIR), Ghaziabad 201002, India

cited whereby calcium alginate has been explored as a packaging material [25–28]. The present study has been conducted to optimize the processing conditions to achieve suitable properties in terms of moisture content, water uptake and swelling ratio, solubilized matter in water, mechanical (tensile) strength, elongation at break, and transmittance. Since the aim of the study is to develop material at par with presently used polythene, Indian Standard IS 2508, "specification for low-density polyethylene film," has been referred to for certain parameters.

2 Materials and methods

LR grade sodium alginate was purchased from Thomas Baker and anhydrous calcium chloride was purchased from Sigma Aldrich. Deionized (DI) water has been used where ever required.

2.1 Film preparation

Five grams of sodium alginate (SA) was dissolved in 100 mL DI water and stirred (at 700 rpm) continuously for 1 h which results in preparation of 0.23 M solution of SA (of almost neutral pH). The solution was coated on a glass surface with the help of a glass rod by placing fine spacers of both sides of the glass to ensure uniformity. The film so formed was allowed to dry for 10 min at room temperature. In the next step, the SA film was allowed to cross-link with $CaCl_2$, to form calcium alginate (CA) films by dipping it into the solution of $CaCl_2$ wherein two different studies were carried out.

(1). $CaCl_2$ samples of varying molarity viz. 0.09, 0.27, 0.45, 0.63, 0.81, 0.99, and 1.17 M were prepared by varying the concentration of $CaCl_2$, i.e., 1%, 3%, 5%, 7%, 9%, 11%, and 13% in water. (The solutions were of almost neutral pH, and were prepared using magnetic stirrer at 700 rpm.) The cross-linked films were removed from the $CaCl_2$ solution (once they left the glass plate) and washed with DI water and then dried in a hot air oven at 45–50 °C for 12 h. The CA film samples prepared by cross-linking with 1%, 3%, 5%, 7%, 9%, 11%, and 13% $CaCl_2$ have been designated as C_1, C_3, C_5, C_7, C_9, C_{11}, and C_{13} respectively.

(2). In the second study, the most appropriate sample from the study (1) was further optimized for the cross-linking time. The samples prepared by varying the cross-linking time as 15 min, 30 min, 45 min, and 60 min have been designated as T_1, T_2, T_3, and T_4 respectively.

The CA films were washed with DI water and then dried in a hot air oven at 45–50 °C for 12 h. Figure 1 shows the schematic for the film preparation.

2.2 Film characterization

Four samples for each film formulation were prepared and characterized at room temperature.

2.2.1 Thickness

A calibrated digital screw gauge with 0.001-mm resolution (MITUTOYO, model MDC-25PX, Japan) was used for the determination of film thickness. The final thickness of a film was measured by taking the average of 12 random measurements from each sample.

2.2.2 FTIR analysis

The effect of IR radiation on the CA films were evaluated by Fourier transform infrared (FTIR) spectroscopy (Nicolet 5700) at room temperature. The analyses have been carried out in the range of 4000–500 cm^{-1} by measuring the transmittance versus wavelength with 12 consecutive scans at a resolution of 64 cm^{-1} [29].

2.2.3 Moisture content

The moisture content of films was determined gravimetrically by taking the weight of the samples before and after heating to 105 °C for 24 h using a vacuum oven [14]. It is expressed as a percentage of the total mass.

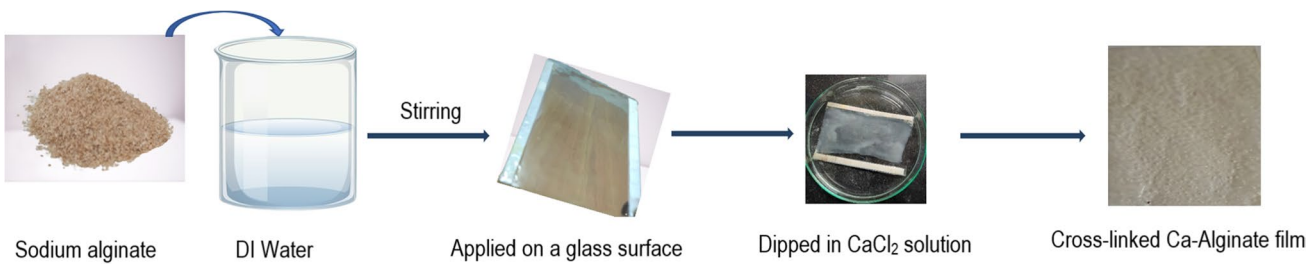

Fig. 1 Schematic for calcium alginate film preparation

2.2.4 Water uptake degree (WU) and swelling ratio (SR)

The methodology proposed by Costa et al. [30] has been used for determining the swelling ratio of the films which is measured as water uptake degree (WU). The initial weight of the films was measured, and the films were immersed in distilled water at 25 °C for an initial time of 2 min. The films were removed and placed between two filter papers for removing excess water present on the surface of the films. The films were weighed and again immersed in the water bath for successive reading at different time durations, i.e., 2, 5, 10, 15, 20, 25, 30, 35, 40, 45, 50, 55, 60, 70, 80, and 90 min.

The SR of the film was determined by varying the temperature of water (25 °C, 35 °C, 50 °C, 70 °C, and 90 °C) in which the films were immersed according to the methods reported by Rhim J. W. et al. [14, 31]. In brief, the pre-weighed sample of the film was immersed in water for 15 min, at a given temperature. After which the films were removed, wiped dry with filter paper, and weighed. SR was expressed as a fraction of the increase in weight against the initial weight of the film.

$$\mathrm{SR} = \mathrm{Wf} - \mathrm{Wi}/\mathrm{Wi} \times 100 \quad (1)$$

where Wf is the final weight and Wi is the initial weight of alginate film.

2.2.5 Solubilized matter in water (S)

The solubilized matter in water was determined using Atomic Absorption Spectroscopy (SHIMADZU, AA, model-AA-7000F, 1.04, S/N-A30925300720, Japan). Samples were prepared by the method proposed by Irissin-Mangata et al. [32]. The results reported are an average of experiments performed on four samples. Initially, the mass (m_i) of each sample was determined (so that it remains constant for each sample) and was immersed at 25 °C with mild shaking (200 rpm) in 50 mL distilled water in a controlled temperature water bath for 24 h. The water sample was collected in a glass bottle after removing the alginate film. The final value was obtained with the equation:

$$\mathrm{S} = \text{Mean of } \mathrm{ABs}/\mathrm{Ws} \times 1/100 \quad (2)$$

where Ws is the weight of the sample and ABs is the absorbance of the sample.

2.2.6 Mechanical characteristics (tensile strength and elongation %)

A universal testing machine (Instron model: 5967) was used for the determination of mechanical properties (tensile strength and elongation %) of the alginate films, according to the standard test method IS 2508 [33]. Span length was set at 50 mm and cross-head speed was set at 0.5 mm/s. Four samples of film strips measuring 50 × 10 mm was tested for each film. The required parameters were directly determined from the stress–strain curves by the stable micro-systems software Texture V.1.15.

2.2.7 Scanning electron microscopy

The morphology of the sample was studied using SEM model: VPSEM Zeiss EVO M-10.

2.2.8 X-ray diffraction

X-ray diffraction studies were performed on Rigaku mini flex Powder X-ray Diffractometer using Cu Kα radiation of 1.5418 Å wavelength. The measurements were carried at the rate of 2^0/min for 2 theta between 5 and 80° at room temperature.

2.2.9 Transparency

Analytical Jena SPECORD 210 plus double beam UV–Vis spectrophotometer was used for transmittance measurements. Samples (of dimensions 1.5 cm × 4 cm) were placed in the cells and measured against the air to measure the light transmittance of the films in the range of 250–800 nm.

2.2.10 Atomic force microscopy

The topography of the samples were studied using atomic force microscope model: Bruker Multimode 8 AFM with Nanoscope V controller.

2.2.11 Biodegradability

For the determination of biodegradation, four samples of each film were placed separately in 3 glass beakers containing black soil, cow dung compost, and soil compost mixture (in 1:1 ratio), with 70–90% moisture at room temperature. The time for decomposition was determined and compared with that of paper and polythene.

Further to study the photodegradation, four pre-dried films of each sample were exposed to sunlight (38 ± 2 °C) at normal atmospheric conditions, and the weight loss was determined.

3 Results

3.1 Study 1: Variation in the concentration of the cross-linking solution

3.1.1 Thickness and density

The average film thickness and density (along with the percent variation), and % moisture values for samples prepared

with varying concentrations of cross-linking solution are given in Table 1. The slight variation in the average thickness of different sample films is probably because of the hand lay-up process used. However, the variation in the thickness of the film of a given sample was less than 20% (except for sample C_{13}) which is acceptable as per IS 2508 (specification for low-density polyethylene film). The standard allows tolerance of ± 25%, if the nominal thickness is ≤ 0.04 mm and ± 20% when the thickness is > 0.04 mm. The variation in thickness have been further ascertained using surface topography studies using atomic force microscopy [34, 35]. The AFM images of samples C_3 and C_{13} as shown in Fig. 2. While C_3 shows uniformity in its thickness, roughness in the surface is clearly visible for sample C_{13}.

The density of the films developed is much less than that of polyethylene with a variation of less than 8% for all the samples (except for C_{13}).

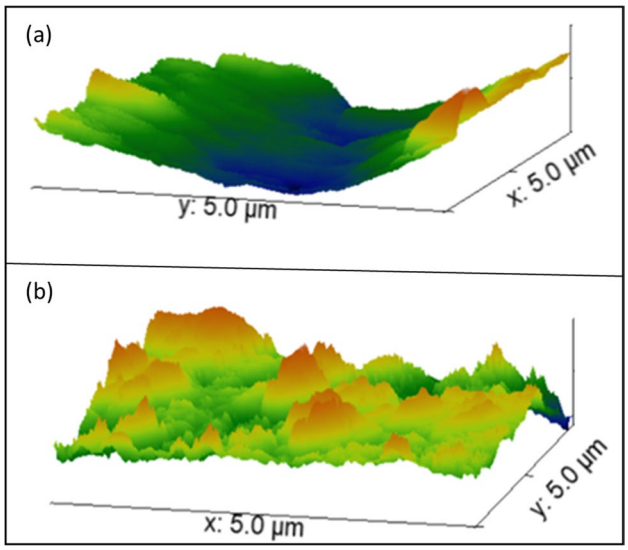

Fig. 2 AFM images of samples **a** C_3 and **b** C_{13}

3.1.2 Moisture content

The moisture content in the samples increases with increasing concentration of $CaCl_2$%, as shown in Table 1. This is probably because all the material does not take part in the reaction. With increasing concentration of the cross-linker, there may be an excess of $CaCl_2$ which is not completely washed off, and because of its sufficient hydrophilic nature, it has the tendency to attract water vapors from the surrounding air, resulting in increased moisture content of the sample.

3.1.3 Water uptake degree (WU) and swelling ratio (SR)

The water uptake degree and swelling ratio of calcium alginate films prepared with varying concentrations of $CaCl_2$ are shown in Fig. 3. From Fig. 3a, the % water uptake increases in samples cross-linked with a higher concentration of $CaCl_2$. However, after 50 min., the water uptake (or the weight change) was negligible. The SR (Fig. 3b) increases in samples prepared with increasing concentration of $CaCl_2$ and is minimal in the case of sample C_3 wherein the sample thickness swells to nearly 15% at 50 °C water temperature and thereafter remains constant. Figure 4 shows the photographs of sample C3 before and after being immersed in water at 25 °C for 30 min., indicating no apparent change in the structure of the CA film.

Water uptake degree and swelling ratio of sample films can be correlated to the presence of the excess amount of $CaCl_2$ on the surface of the film. Due to the hydrophilic nature of the later, film samples absorbed water and results in increased SR and WU [36].

3.1.4 Solubilized matter in water

Solubilized matter in water can be viewed as a measure of total excess materials, which are dissolved in water from the film. The results of the AAS (atomic absorption spectroscopy) study shows that the solubilized matter in water increases with increasing $CaCl_2$ concentration during sample preparation as shown in Fig. 5. As already mentioned, it is probably due to excess $CaCl_2$ on the surface of the prepared sample that leaches out when the film is dipped into water.

Table 1 Thickness, density and moisture % of CA films prepared by varying the concentration of calcium chloride

Sample ID	Avg. thickness (mm)	Thickness variation %	Average density (g/cm^3)	Density variation %	Moisture %
C_1	0.043 ± 0.003	11.6%	0.152 ± 0.001	6.4%	5.04%
C_3	0.045 ± 0.005	11.1%	0.151 ± 0.001	6.6%	5.01%
C_5	0.044 ± 0.003	6.8%	0.142 ± 0.001	7.1%	5.44%
C_7	0.041 ± 0.009	11.9%	0.160 ± 0.002	7.1%	6.12%
C_9	0.048 ± 0.006	12.5%	0.144 ± 0.001	7.1%	6.89%
C_{11}	0.040 ± 0.006	15%	0.140 ± 0.001	7.5%	7.22%
C_{13}	0.042 ± 0.010	23.8%	0.132 ± 0.001	8.6%	9.16%

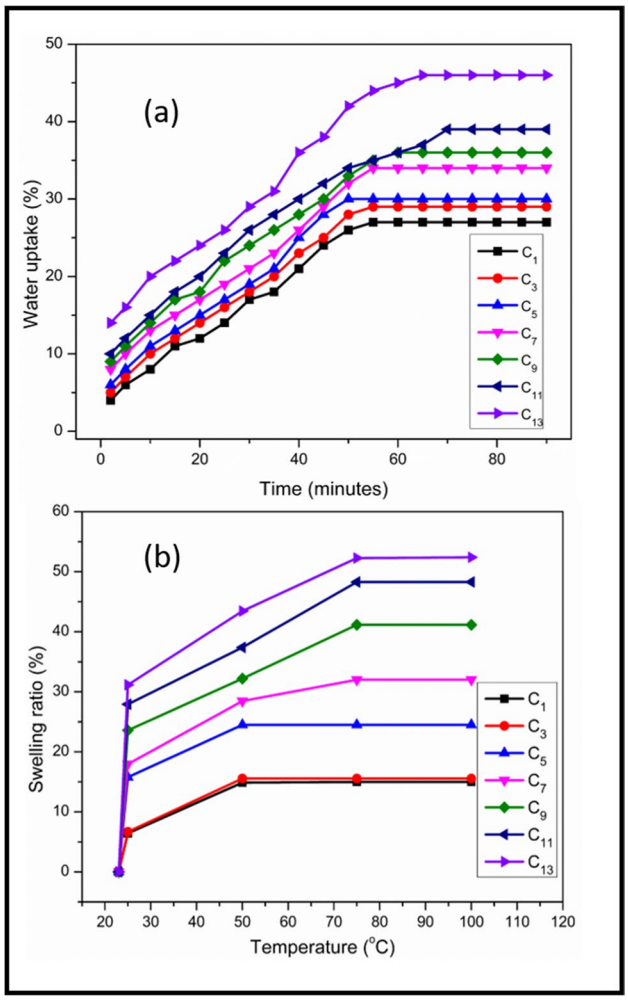

Fig. 3 **a** Water uptake degree and **b** swelling ratio of Ca-alginate films cross-linked with different concentrations of calcium chloride

3.1.5 Mechanical characteristics (tensile strength and elongation percentage)

The results of the tensile strength and % elongation at the break of the samples is shown in Fig. 6a while the stress–strain curves are shown in Fig. 6b. Both parameters are important for packaging materials. The strength of the films is primarily due to the cross-linking reaction (by ionic bridging) between the carboxyl groups of two adjacent polymer chains of sodium alginate with the Ca^{+2} ions. Sample C_1 shows very low strength probably due to incomplete cross-linking of the sample. Sample C_3 shows the highest value of tensile strength, i.e., 11.65 ± 0.20 MPa, which is in close proximation to that of 11.77 MPa required for LDPE per IS 2508. The sample (C_3) shows maximum elastic behavior as compared to samples C_5 and C_7. The elastic region for C_9–C_{13} is minimum. All the samples show a ductile nature. The area under the curve is a measure of toughness and is found to be maximum for C_3. However, the elongation percentage for sample C_3 is 70% which is slightly less than the required 100% as per the standard [33]. The tensile strength and elongation % decreased successively with the increasing $CaCl_2$ concentration from C_3 to C_{13}. This decrease can further be attributed to increase in the non-uniformity of the samples (which may act as crack-initiator) and also the increase in the moisture content of the samples. Such a trend is also exhibited by natural fibers/polymer hybrid composites [37–39].

3.1.6 Transparency

The results of the transmittance by the samples are shown in Fig. 7. The CA film prepared with 3% $CaCl_2$ showed high transmission of light, but from samples C_3 to C_{13} (prepared with increasing concentration of $CaCl_2$), the light transmittance of alginate films reduces successively at all the wavelengths. This is because surface roughness greatly affect the

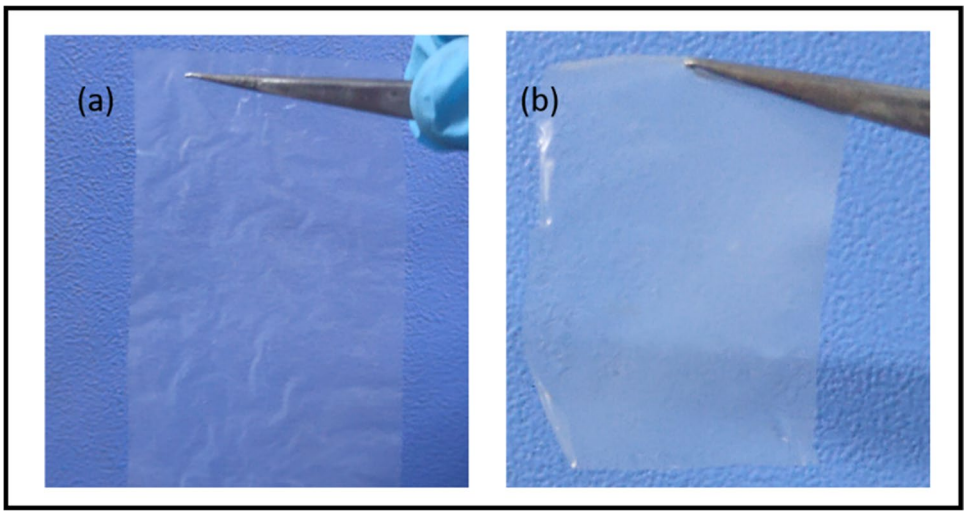

Fig. 4 Photographs of sample C3 **a** before and **b** after being immersed in water at 25 °C for 30 min

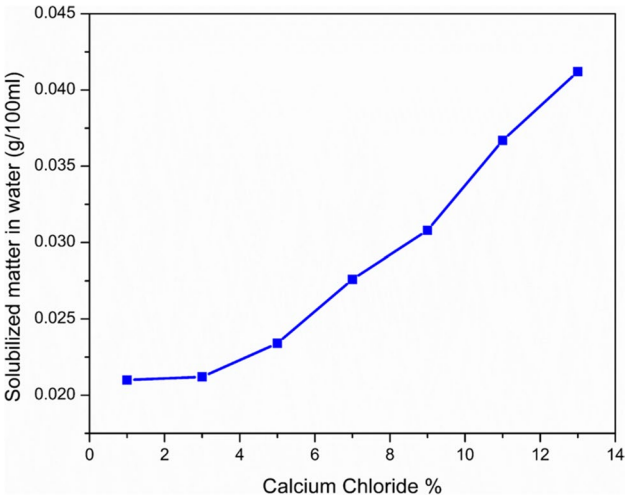

Fig. 5 Variation in the solubilized matter in the water of samples prepared with different $CaCl_2$ concentrations

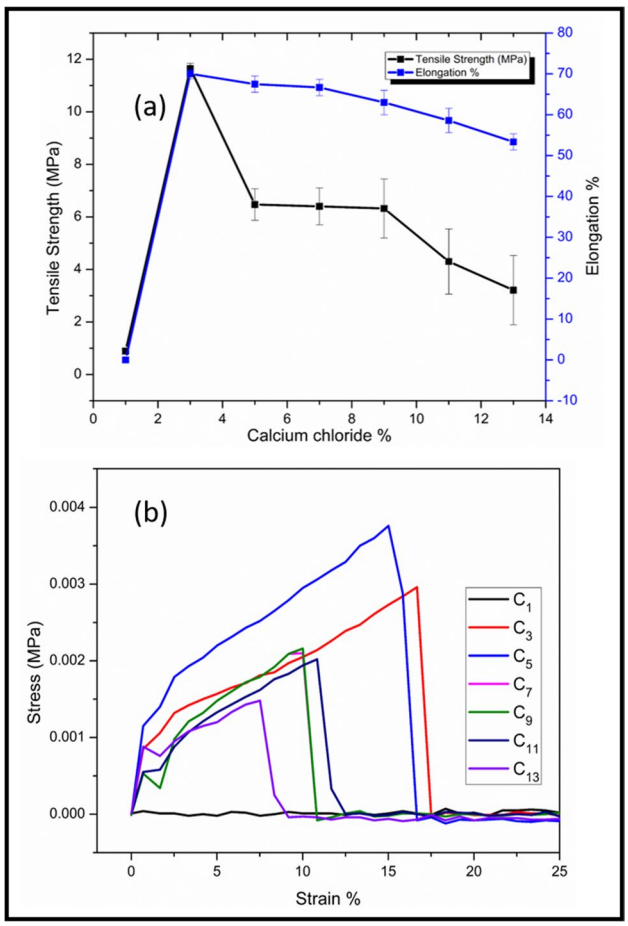

Fig. 6 Variation in the **a** tensile strength and % elongation at break and **b** stress vs. strain curves for the CA films cross-linked with different $CaCl_2$ concentrations

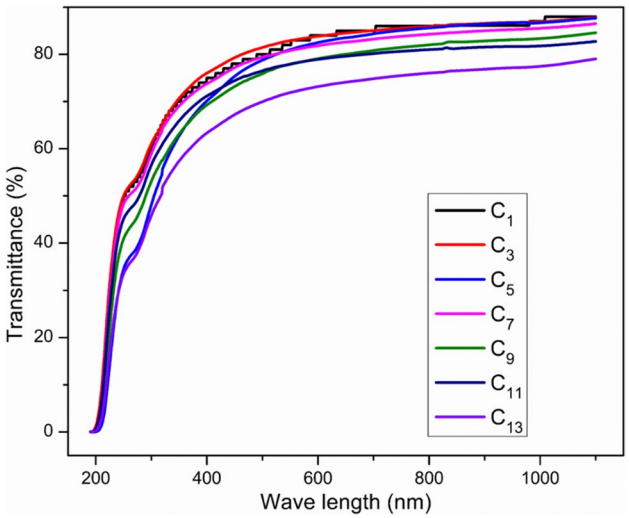

Fig. 7 The transmittance of CA films prepared with different concentrations of $CaCl_2$

transmittance of CA films. As already shown by the AFM data in Sect. 3.1.1, the variation in thickness and hence the surface roughness is much higher for sample C_{13} than in C_3 leading to the decrease in transmittance of the former.

3.1.7 Biodegradability

Biodegradability is an important parameter for determining the material's usefulness as an environment-friendly packaging material. Fungi, algae, and bacteria are important organism in the biodegradation process [40]. The degradation of the natural polymer takes place via oxidation and hydrolysis, whereby it degrades into CO_2 and biomass [41]. Hence, a moisture level of 70–90% was maintained in the degradation media (black soil, cow dung compost, and the mixture). After every 12 h, the film was taken out from the respective media and weighed. Weight loss (WL) was obtained using the following equation:

$$WL\% = (W_i - W_f) \times 100 \quad (3)$$

where WL is the weight loss, W_i is the initial, and W_f is the final weight of the film. The results are summarized in Table 2.

3.2 Study 2-Variation in the cross-linking time

From the above analysis, samples prepared with 3% $CaCl_2$ were selected for further studies owing to their reduced water adsorption and increased strength as compared to other samples.

3.2.1 Thickness, density, and moisture content

The average film thickness and density (along with the percent variation) and % moisture of samples prepared by varying the cross-linking times are shown in Table 3. The thickness variation

Table 2 Degradation time of CA films prepared by varying the concentration of CaCl2 in different media

Sample ID		C_1	C_3	C_5	C_7	C_9	C_{11}	C_{13}
Initial weight taken (g)		0.209	0.219	0.220	0.210	0.231	0.212	0.214
Degradation time (hour) in different media	Black soil	278	290	444	468	492	504	528
	Cow dung compost	114	120	132	156	180	204	236
	Soil and compost mixture (1:1)	210	220	432	456	480	492	516

Table 3 Thickness, density, and moisture % of CA films developed by varying the cross-linking time

Sample ID	Avg. thickness (mm)	Thickness variation %	Average density (g/cm^3)	Density variation %	Moisture %
T_1	0.032 ± 0.003	9.3%	0.151 ± 0.001	0.66%	6.01%
T_2	0.035 ± 0.004	11.4%	0.142 ± 0.001	0.70%	5.44%
T_3	0.038 ± 0.004	10.5%	0.158 ± 0.001	0.63%	5.12%
T_4	0.036 ± 0.004	11.1%	0.144 ± 0.001	0.69%	4.99%

of the film of a given sample was less than 20%, which is acceptable as per IS 2508. The cross-linking time did not have any effect on the sample thickness. Moreover, the variation in density of the samples is much less as compared to those prepared in study 1. Thus, when sufficient time is given for the samples to cross-link, greater uniformity is achieved in the sample.

The moisture content decreases with increasing cross-linking time from sample T_1 to T_4 as shown in Table 3.

3.2.2 Water uptake degree and swelling ratio

The water uptake degree (Fig. 8a) and the swelling ratio (Fig. 8b) decreased with the increase in cross-linking time from sample T_1 to T_4. It is the measure of the stability of the samples when in contact with water. For sample T_1, the WU and hence the SR are maximum. This is probably because cross-linking is not complete in 15 min, and some of the sodium alginate remains unreacted. Sodium alginate is a hydrophilic polysaccharide and has the tendency to uptake water. With increasing cross-linking time, the sodium alginate films achieve complete polymerization/cross-linking with calcium, and the absence of any unreacted sodium alginate on the surface probably imparts increased stability, and hence, the WU and the SR decrease.

3.2.3 Solubilized matter in water

The solubilized matter in water (as determined from AAS) decreased with increasing cross-linking time from T_1-T_4 as shown in Fig. 9. The explanation as given in Sect. 3.2.2 justifies the finding. With increasing cross-linking time, maximum amount of water-soluble sodium alginate is cross-linked to water insoluble calcium alginate. Due to this action, concentration of unreacted sodium alginate decreases resulting in a sharp decline in solubilized matter in water from T_1 to T_4.

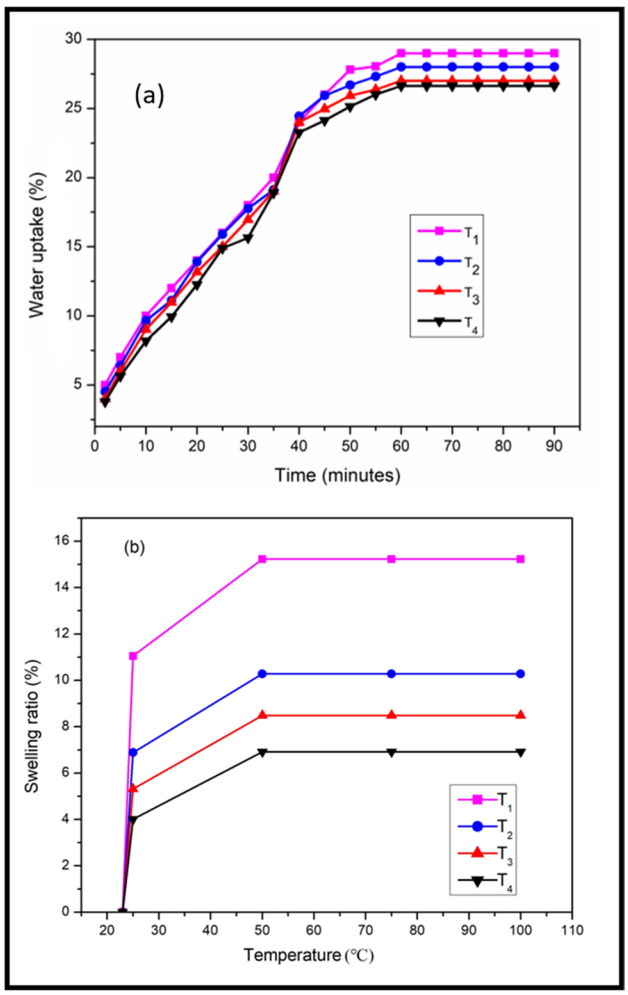

Fig. 8 **a** Water uptake degree and **b** swelling ratio of CA films immersed in distilled water at 25 °C at different cross-linking times

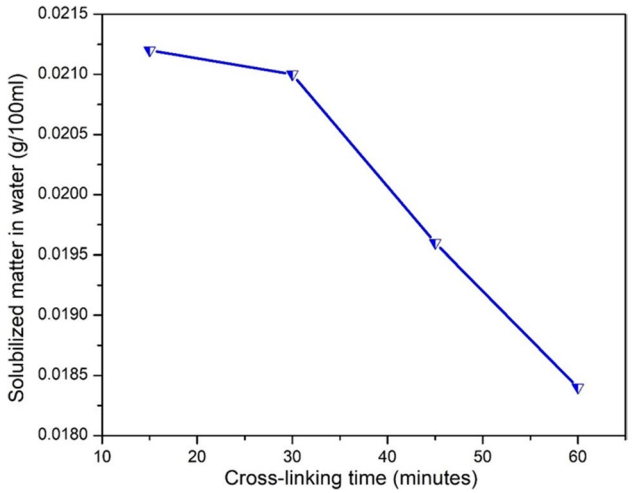

Fig. 9 Solubilized matter in water with different cross-linking times

3.2.4 Mechanical characteristics (tensile strength and elongation %)

Mechanical parameters of the calcium alginate films prepared with increasing cross-linking time are summarized in Fig. 10. The strength and % elongation (as shown in Fig. 10a) increase with increasing cross-linking time from 15 to 30 min and thereafter decreases. This suggests that complete cross-linking has been achieved in 30 min. However, further exposure to the cross-linking solution may cause some non-uniformity in the sample, which may act as crack initiators when the sample is subjected to load. Similar results have been reported by Chavez MS et al. [42].

From the stress–strain curve of the samples, sample T_1 shows maximum elastic region probably due to reduced cross-linking. Furthermore, the elastic region decreases in samples T_2, T_3, and T_4. All the samples exhibit ductile nature with maximum elongation/ductility for sample T_2. The area under the curve which is also a measure of toughness of the sample is highest for sample T_2.

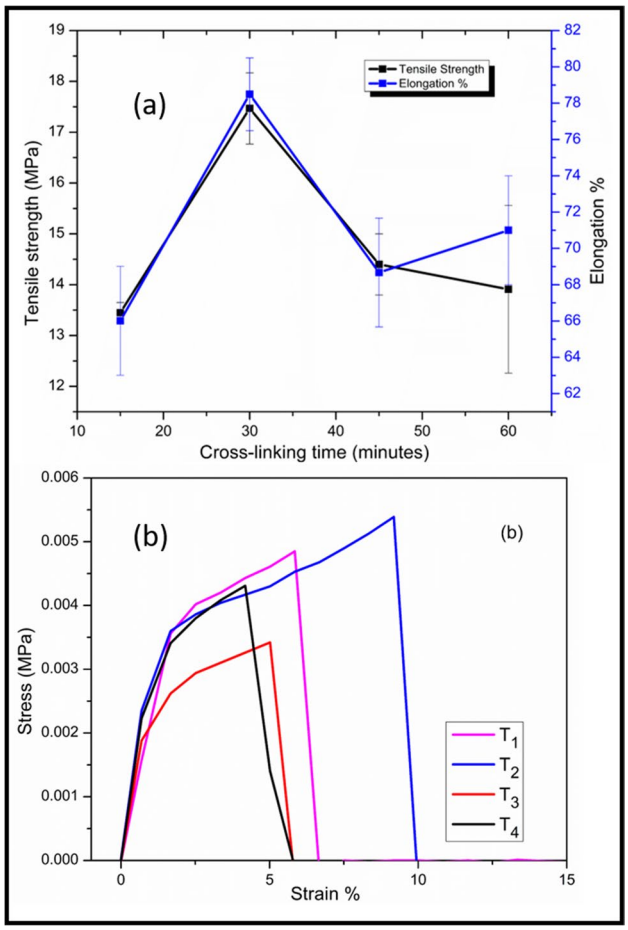

Fig. 10 Variation in the **a** tensile strength and elongation % with cross-linking time, **b** stress vs strain curve

The SEM images of the fractured part of sample T2 are shown in Fig. 11. Figure 11b is the magnified view of the highlighted portion of Fig. 11a. The morphology of the fractured surface is not smooth but irregular and slightly porous in nature (as is expected in case of bio-materials). This indicates towards good packaging efficiency of the material by providing cushioning effect.

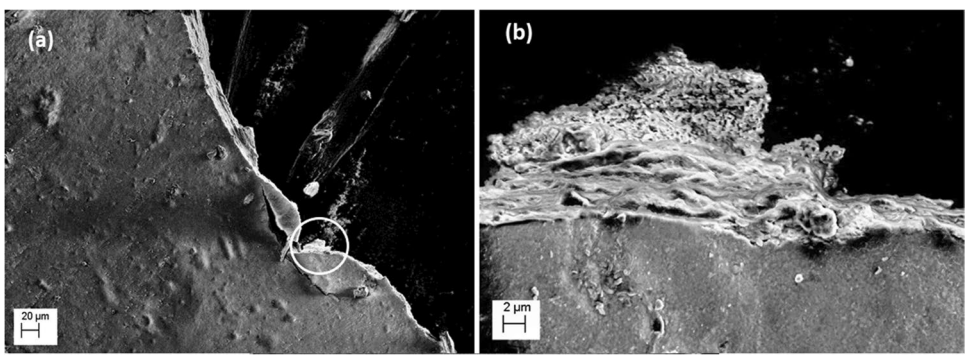

Fig. 11 SEM images of the fractured part of sample T_2

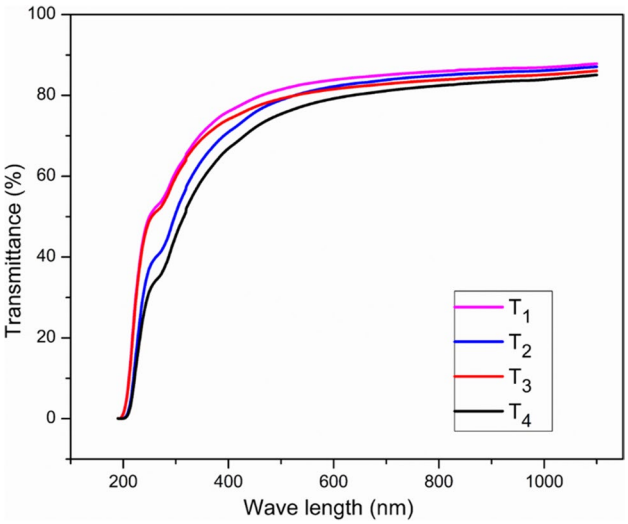

Fig. 12 Transmittance of CA films with various cross-linking time

3.2.5 Transparency

The film samples show high transmittance for visible light as shown in Fig. 12. It is interesting to note that the transmittance of the visible light toward the alginate film did not change significantly with different cross-linking times. However, as already mentioned in Sect. 3.2.4, excessive exposure to the cross-linking solution may render the films non-uniform leading to a decrease in transparency. Thus, the CA film can be used as a see-through packaging film [43–45], with a visible light transmittance of more than 80%.

3.2.6 Infrared treatment

Processing of food products is necessary for extending their safety and shelf life. Infrared (IR) heating is a contactless, chemical-free, economical, and easy method that

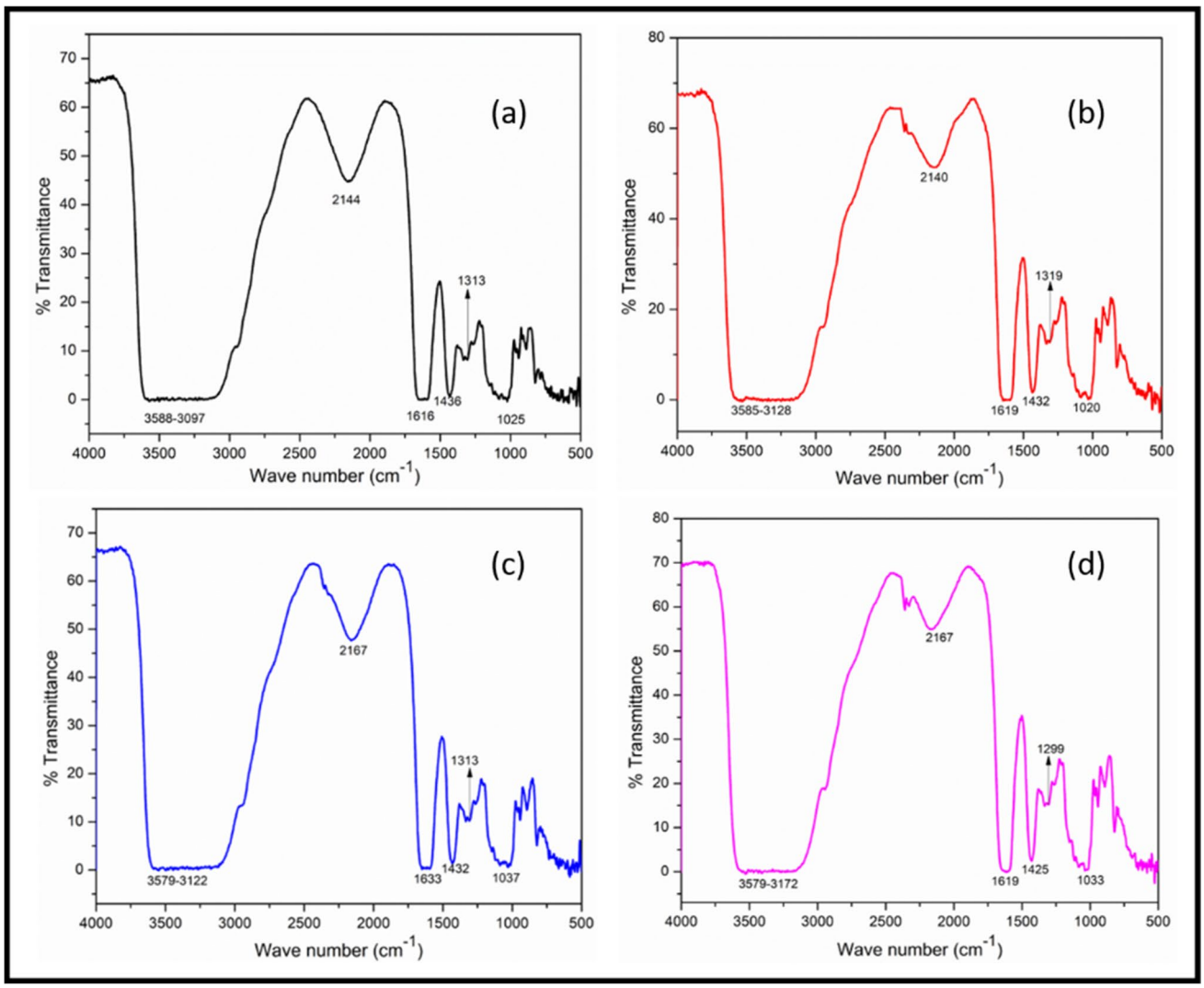

Fig. 13 FTIR analysis of calcium alginate film (sample T2) **a** without treatment; **b** after 30 s of IR treatment; **c** after 1 min of IR treatment; **d** after 2 min of IR treatment

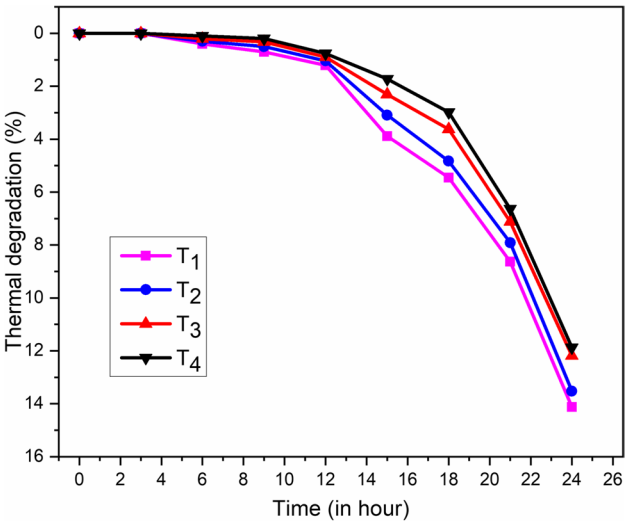

Fig. 14 Photodegradation of CA films with various cross-linking times

has been used widely for disinfecting the food items. As a potential material for food packaging, the optimized CA film (T_2) was subjected to IR radiation (for 30 s, 1 min, and 2 min), and the effect of the same was analyzed via FTIR spectroscopy. The FTIR spectra of CA before and after IR treatment has been shown in Fig. 13.

The FTIR spectra displays important absorption bands of various functional group. The absorption band at 3588–3097 cm^{-1} is due to the hydrogen bonded or alcoholic hydroxyl groups (-OH) [36]; the stretching vibration of the ketene group was observed at 2150 cm^{-1} [46]; the strong band at 1633–1619 cm^{-1} is due to C = C stretching of alkene and strong peak at around 1430 cm^{-1} corresponds to C-H bending of alkane. Band at 1313–1250 indicates C-O stretching of aromatic ester, and several peaks in the range of 1200–1020 cm^{-1} correspond to C–OH stretching [47–51]. The FTIR peak observed at 900–930 cm^{-1} [52] and 827–835 cm^{-1} relates to the C-H bending and asymmetric -CH_2 [52]. As is clear from the curves, not much change was observed on the sample by 2 min of IR treatment, thus suggesting that it can be safely used for IR treatment of the packaged food with deterioration. The small peak arising at around 2167 cm^{-1} corresponds to O = C = O stretching

Table 5 Comparison of biodegradability of CA film, paper, and polythene in cow dung compost

Samples	CA film (T_2)	Paper	Polythene
Weight (gm)	0.213	0.210	0.160
Thickness (mm)	0.047	0.010	0.039
Degradation time (in hour)	198	260	Did not degrade

which is just due to background noise probably arising out of atmospheric CO_2 [53].

3.2.7 Photodegradation

The degradation of the samples (when subjected to sunlight) has been shown w.r.t. weight loss of the samples over a period of 24 h (Fig. 14), and correspondingly, the curve has been divided into 3 stages. The first stage shows a very slight weight loss, probably due to the removal of water. Substantial weight loss is shown in the second stage, in which probably due to the start of breakage of ether-ether linkages (ether being the weakest bond) in the presence of sunlight. Therefore, the polymer chains have broken into monomer chains. In stage three, photodegradation has increased due to the presence of fewer polymeric bonds.

Overall, photodegradation has decreased with increased cross-linking time from sample T_1-T_4 because of the maximum polymer covalent and ionic bond formation by higher cross-linking time.

3.2.8 Biodegradability

The biodegradability of the samples was also tested as per the method described in Sect. 2.2.8. With the increase in the cross-linking time from samples T_1-T_4, the degradation time slightly increased as summarized in Table 4. This may be due to an increased cross-linking reaction. Furthermore, no change in degradation time from T_2 to T_3 probably suggests that the reaction is complete in 30 min.

Table 4 Biodegradability of CA film prepared by varying the cross-linking time

Sample ID		T_1	T_2	T_3	T_4
Weight (g)		0.210	0.221	0.213	0.211
Degradation time (hours) in different media	Black soil	290	302	302	324
	Cow dung compost	160	184	184	196
	Soil and compost mixture (1:1)	180	204	204	228

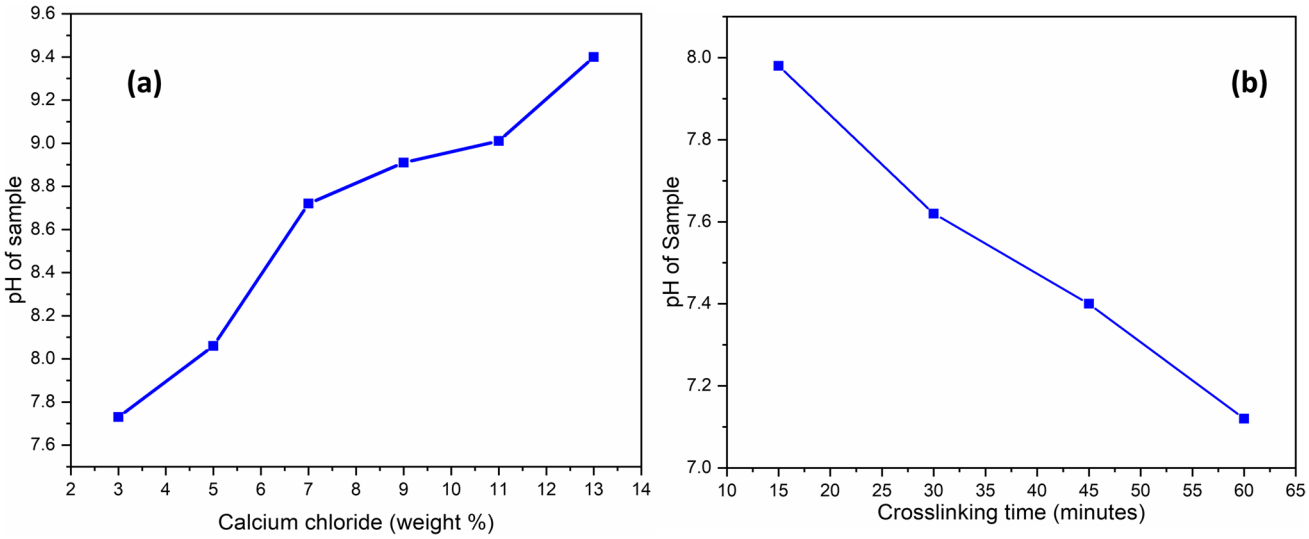

Fig. 15 The pH of the water after immersing CA films with **a** variation in calcium chloride concentration and **b** variation in cross-linking time

Furthermore, a comparison showed that the biodegradability of CA film (T_2) is faster than paper (80 GSM) and polyethylene in the compost (Table 5).

4 Discussion

To explain the results of study 1, the CA films were dipped and stirred in distilled water at atmospheric temperature and pressure, for 30 min after which the films were removed and the pH of the water was measured. It was found to increase as shown in Fig. 15a [54]. This was probably due to the presence of excess unreacted Ca^{+2} on the film surface, which is hydrophilic and produced hydroxide with reaction from water, which might have resulted in increasing the pH value of distilled water.

The increase in the total solubilized matter in water with increasing $CaCl_2$% is due to the presence of the excess amount of unreacted $CaCl_2$ on the surface of the film. The increase in moisture content, water uptake degree, and swelling ratio of the sample films [36] may be attributed to the same reason. Furthermore, since the samples were removed once they left the glass plate, the samples dipped in a lower concentration of $CaCl_2$ led to a longer reaction period as compared to samples prepared by dipping in higher concentrations of the cross-linking solution. Thus, the slow reaction

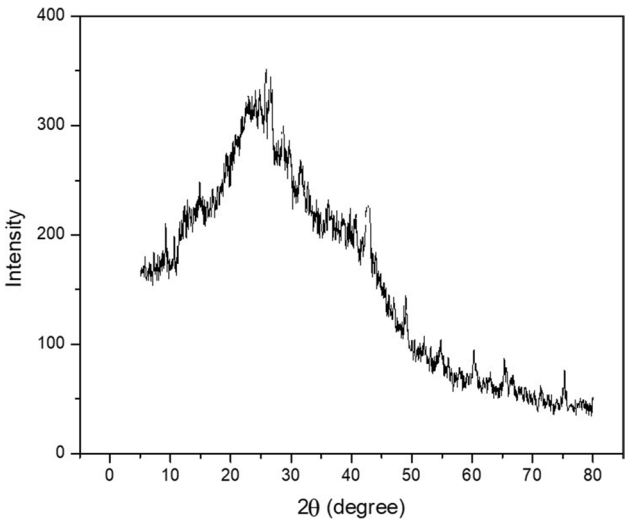

Fig. 16 XRD pattern of CA film

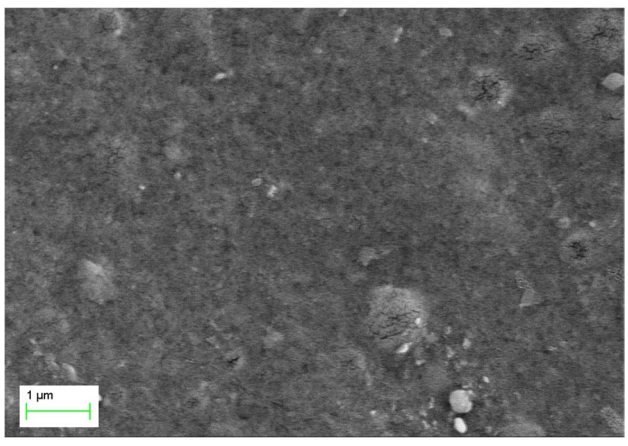

Fig. 17 SEM image of CA film

probably led to a more uniform sample with reduced voids and hence also led to improved strength. The increase in the variation of thickness and density for sample C_{13} also points towards the decrease in uniformity of the CA films with the increase in the concentration of $CaCl_2$, as is also clear by the AFM images as shown in Fig. 2. The increase in the degradation time with an increase in the concentration of the cross-linking solution may also be due to the presence of excess $CaCl_2$ on the surface of the film since $CaCl_2$ behaves as an inhibitor for the micro-organisms [55].

Further in study 2, since the concentration of the cross-linking solution is low (3%), complete polymerization takes time. Hence, for the samples prepared with increased cross-linking time, the unreacted sodium alginate on the surface reduce as compared to sample T_1 and the moisture content also decreases. For the same reason, other parameters like solubilized matter in water and WU are also reduced.

To further ascertain the presence of free Ca ions on the film surface, the films were dipped in water for 30 min with constant stirring and the pH of the supernatant liquid was determined (as shown in Fig. 15b). The pH of all the supernatant liquids is basic and the reduction in its value is probably the result of the reduction in the free Na ions present on the surface.

The X-ray diffraction pattern of the CA film (T_2) is shown in Fig. 16. Weak diffraction peaks are obtained at 2 theta values 14.8° and 25°, which indicated towards amorphous nature of the material. The SEM image in Fig. 17 shows the surface morphology of the sample, which is quite uniform and fibrous indicating its potential as a biodegradable packaging material.

5 Conclusion

Calcium alginate (CA) films have been successfully prepared, whereby the concentration of the cross-linking solution and the cross-linking time was found to greatly affect the properties of the developed films. Different characterizations show that a lower concentration of $CaCl_2$ (3%) with 30 min of optimized cross-linking time leads to the development of uniform CA film and therefore showed better properties. It further gives us an indication as to how the film properties can further be tailored as per specific requirements. Above all the CA films are fast biodegradable (in soil, compost, and sunlight) as compared to presently used materials and must be explored as packaging materials for food and other items. The scope of research in this field involves further reducing the water uptake and swelling of the samples and increasing their mechanical strength that can be done by addition of suitable additives like bio-polymers and nanomaterials. There is also a possibility to make it anti-bacterial for specific applications.

Acknowledgements The authors are grateful to the Director, NPL, for providing the necessary research facilities and permission to publish results and CSIR for providing the research funds. The authors would also like to thank S.S. Sharda for mechanical testing, Sachin Yadav for FTIR analysis, and Shrawan Kumar for the study of solubilized matter in water by using the AAS technique.

Author contribution Omkar Saswat has performed the experiments and performed all characterization. Omkar Saswat also prepared the first draft of the manuscript and contributed to the optimization of various characterizations. Priyanka H. Maheshwari conceptualized and supervised the study and contributed to data interpretation and discussion. She also edited the various drafts of the manuscript.

Funding The work is supported by CSIR-National Physical Laboratory, New Delhi.

Declarations

Competing interests The authors declare no competing interests.

References

1. F. Ribeiro, J.W. O'Brien, T. Galloway, K.V. Thomas, TrAC Trends Anal. Chem. **111**, 139–147 (2019)
2. R. Rizal, L.M. Tua, S.B. Ginting, J. Phys. Conf. Ser. **1569**, 032016 (2020). https://doi.org/10.1088/1742-6596/1569/3/032016
3. K. Petersen, P. Vaeggemose Nielsen, G. Bertelsen, M. Lawther, M.B. Olsen, N.H. Nilsson, G. Mortensen, Trends. Food. Sci. Technol. **10**, 52–68 (1999)
4. A. Riley, Fundam. Mater. Process. (2012). https://doi.org/10.1533/9780857095701
5. S. Benavides, R. Villalobos-Carvajal, J.E. Reyes, J. Food Eng. **110**, 232–239 (2012)
6. A. Saarai, T. Sedlacek, V. Kasparkova, T. Kitano, P. Saha, J. Appl. Polym. Sci. **126**, E79 (2012)
7. J. Wang, J. Wei, S. Su, J. Qiu, S. Wang, J. Mater. Sci. **50**, 5458–5465 (2015)
8. F. Debeaufort, J.-A. Quezada-Gallo, A. Voilley, Crit. Rev. Food Sci. **38**, 299–313 (1998)
9. F. Lü, X. Ye, D. Liu, Nongye Jixie Xuebao/Trans. Chin. Soc. Agric. Mach. **40**, 138–142 (2009)
10. Q. Xiao, Q. Tong, L.T. Lim, Carbohyd. Polym. **87**, 1689–1695 (2012)
11. J. Li, J. He, Y. Huang, D. Li, X. Chen, Carbohyd. Polym. **123**, 208–216 (2015)
12. A. Konwar, D. Chowdhury, RSC Adv. **5**, 62864–62870 (2015). https://doi.org/10.1039/c5ra09887d
13. F. Nan, J. Wu, F. Qi, Y. Liu, T. Ngai, G. Ma, Colloids Surf., A **456**, 246–252 (2014)
14. J.W. Rhim, LWT Food Sci. Technol. **37**, 323–330 (2004)
15. J.S. Yang, Y.J. Xie, W. He, Carbohydr. Polym. **84**, 33–39 (2011)
16. X. Guo, Y. Wang, Y. Qin, P. Shen, Q. Peng, Int. J. Biol. Macromol. **162**, 618–628 (2020)
17. K.I. Draget, C. Taylor, Food Hydrocolloids **25**, 251–256 (2011)
18. Y. Qin, J. Jiang, L. Zhao, J. Zhang, F. Wang, Biopolymers for Food Design, 409–429 (2018).
19. Applications of Alginates in Food. By I. A. Brownlee, C. J. Seal, M. Wilcox, P. W. Dettmar, J. Pearson, (Springer, Berlin, 2009) P., 211–228.
20. R.G. Puscaselu, A. Lobiuc, M. Dimian, M. Covasa, Polymers **12**, 1–30 (2020)

21. M. A. Masuelli, C. O. Illanes, Int. J. BioMater. Sci. Eng. **1**, 1–11 (2014). http://www.openscienceonline.com/journal/biom.
22. A. Fazilah, M. Maizura, A. Abd Karim, K. Bhupinder, B. Rajeev, U. Uthumporn, S.H. Chew, Int. Food Res. J. **18**, 1027–1033 (2011)
23. M.E. Valentine, B.D. Kirby, T.R. Withers, S.L. Johnson, T.E. Long, Y. Hao, J.S. Lam, R.M. Niles, H.D. Yu, Microb. Biotechnol. **13**, 162–175 (2020)
24. I.D. Hay, Y. Wang, M.F. Moradali, Z.U. Rehman, B.H.A. Rehm, Environ. Microbiol. **16**, 2997–3011 (2014)
25. S. Roger, D. Talbot, A. Bee, J. Magn. Magn. Mater. **305**, 221–227 (2006)
26. R. Theagarajan, S. Dutta, J. A. Moses, C. Anandharamakrishnan, Alginates: Applications in the Biomedical and Food Industries, 205–232 (2019).
27. M.G. Kontominas, Foods (2020). https://doi.org/10.3390/foods9101440
28 M.S. Abdel Aziz, H.E. Salama, M.W. Sabaa, Lwt **96**, 455–460 (2018)
29. R. Muthuraj, M. Misra, A.K. Mohanty, ACS Sustain. Chem. Eng. **3**, 2767–2776 (2015)
30. M.J. Costa, M.A. Cerqueira, H.A. Ruiz, C. Fougnies, A. Richel, A.A. Vicente, J.A. Teixeira, M. Aguedo, Ind. Crops Prod. **66**, 305 (2015)
31 J.W. Rhim, A. Gennadios, C.L. Weller, C. Cezeirat, M.A. Hanna, Ind. Crops Prod. **8**, 195–203 (1998)
32. J. Irissin-Mangata, G. Bauduin, B. Boutevin, N. Gontard, Eur. Polymer J. **37**, 1533–1541 (2001)
33. Bureau of Indian Standards (IS 2508), Polyethylene films and sheets (IS 2508 : 2016), Bur. Indian Stand. (2016).
34. R.R. Awasthi, B. Das, Optik (2019). https://doi.org/10.1016/j.ijleo.2019.162973
35. R. R. Awasthi, K. Asokan, B. Das, Appl. Phys. A: Mater. Sci. Process. **125** (2019).
36. J.H. Kim, J.Y. Kim, Y.M. Lee, K.Y. Kim, J. Appl. Polym. Sci. **45**, 1711–1717 (1992)
37. V. Chaudhary, R. Sahu, A. Manral, F. Ahmad, Mater. Today: Proc. **25**, 857–861 (2019)
38. A.A. Bachchan, P.P. Das, V. Chaudhary, Mater. Today: Proc. **49**, 3403–3408 (2020)
39. V. Chaudhary, F. Ahmad, J. Reinf. Plast. Compos. **39**, 572–586 (2020)
40. A. E.-G. TM, I. A. Masmali, J. Plant Pathol. Microbiol. **07** (2016).
41. Fungal Cellulases Production for Biodegradation of Agriculture Waste. By N. Srivastava, M. Srivastava, A. Manikanta, P. W. Ramteke, R. L. Singh, P. K. Mishra, S. N. Upadhyay, 75–89 (Springer, Ukraine 2018).
42. M.S. Chavez, J.A. Luna, R.L. Garrote, J. Food Sci. **59**, 1108–1110 (1994)
43. L.F. Wang, J.W. Rhim, Int. J. Biol. Macromol. **80**, 460–468 (2015)
44. F. Mady, S. Ibrahim, M. Abourehab, J. Adv. Biomed. Pharm. Sci. **4**, 111–118 (2021)
45. R. Pereira, A. Tojeira, D.C. Vaz, A. Mendes, P. Bártolo, Int. J. Polym. Anal. Charact. **16**, 449–464 (2011)
46. J. Yu, J. Wang, Y. Jiang, Nucl. Eng. Technol. **49**, 534–540 (2017)
47. J. Han, Z. Zhou, R. Yin, D. Yang, J. Nie, Int. J. Biol. Macromol. **46**, 199–205 (2010)
48. S. Bajpai, S. Sharma, React. Funct. Polym. **59**, 129–140 (2004)
49. Z. Dong, Q. Wang, Y. Du, J. Membr. Sci. **280**, 37–44 (2006)
50. B. Sarmento, D. Ferreira, F. Veiga, A. Ribeiro, Carbohyd. Polym. **66**, 1–7 (2006)
51. T. Mimmo, C. Marzadori, D. Montecchio, C. Gessa, Carbohyd. Res. **340**, 2510–2519 (2005)
52 A. PietropolliCharmet, P. Stoppa, R. Visinoni, S. Giorgianni, G. Nivellini, Mol. Phys. **100**, 3529–3534 (2002)
53. X. Wang, Y. Hu, L. Song, W. Xing, H. Lu, J. Anal. Appl. Pyrol. **92**, 164–170 (2011)
54. A.A. Badwan, A. Abumalooh, E. Sallam, A. Abukalaf, O. Jawan, Drug Dev. Ind. Pharm. **11**, 239–256 (1985)
55. A.U. Alahakoon, D.D. Jayasena, S. Jung, H.J. Kim, S.H. Kim, C. Jo, Korean J. Food Sci. Anim. Resour. **34**, 221–229 (2014)